Fluorescent Probes

DOI: 10.1002/anie.201205628

DNA Detection Based on Fluorogenic Nanospheres**

*Xin Shu, Yonghui Liu, and Jin Zhu**

An effective molecular diagnostic system generally requires the amplification of either target or signal.[1] Target amplification provides the ability to achieve an extremely high sensitivity. However, the only system that has been worked out thus far is DNA, which can be exponentially duplicated using polymerase chain reaction (PCR) technology.[2] The use of PCR in diagnostics also highlights several major problems, including the complexity of analysis, sensitivity to contamination, and a narrow dynamic range, among others.[3] For a target other than DNA, signal amplification is necessary because the sensitivity is limited by the generally low binding constant of the recognition event. Taken together, the development of a generic diagnostic technique typically favors signal amplification as the method of choice. In this regard, reactivity-based amplification[4] (for example, enzymatic catalysis for enzyme-linked immunosorbent assay[5]) has been the driving force behind many of the currently in-use diagnostic methods. However, the robustness of the assay can be compromised by the inherent instability and variability associated with the reaction center (for example, the enzyme catalysis center).[6] A more straightforward signal amplification strategy could, in principle, be created by the translation of a single binding event into the capture of a multitude of intact signaling labels, without the involvement of any further chemical transformation.[3a,7] One such format exploits directly the signal generated from the collection of labels on a carrier for readout. This kind of direct readout might not be ideal because of the undesired effect (for example, fluorescence quenching) that can result from such closely packed labels. Also, the number of labels that can be accommodated on one carrier is restricted to the available internal space or sites on the surface. We envisioned that a new diagnostic strategy, with enormous signal amplification, would be possible if 1) a nanostructured probe could be directly assembled from the desired label, and 2) the liberation of numerous labels in the nanostructured probe in response to each binding event is highly efficient and reliable.

Building upon our expertise in molecular diagnostics,[8] herein, we report on a sensitive, selective, and multiplexed fluorogenic-nanosphere (FNS) assay for the on-chip detection of DNA (Figure 1). This method takes advantage of a unique fluorescent property associated with a novel FNS formed by

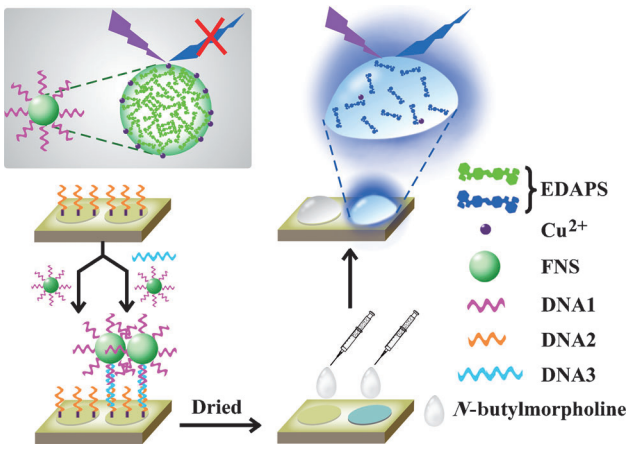

Figure 1. Scheme of FNS-based DNA detection. Gray box: latent **DNA1**-FNS probe, with the fluorescence of EDAPS molecules quenched by substoichiometric amounts of Cu^{2+} ions. A glass slide spotted with **DNA2** is allowed to react with **DNA1**-FNS in either the absence or presence of target **DNA3**. A grayish-blue spot, comprised of a layer of captured **DNA1**-FNS, is generated only when **DNA3** is co-hybridized with **DNA1**-FNS and surface-anchored **DNA2**. The amplified fluorescence signal is achieved through the dissolution of FNSs and release of EDAPS upon incubation with *N*-butylmorpholine.

E-4,4′-di[*N*-(2-aminophenyl)amino]stilbene (EDAPS) and Cu^{2+}.[9] The fluorescence of EDAPS is quenched in the FNS solid state by substoichiometric amounts of Cu^{2+} ions, but can be switched on by the dissolution of the constituent components of FNSs into the surrounding liquid. By holding a large number of EDAPS, FNSs can therefore function as latent fluorophore probes for the binding of any target structure with the capability to amplify the signal. The high quantum yield demonstrated for this class of arylamino-substituted stilbene molecules ensures a good fluorescent readout with EDAPS.[10] A detection limit of 50 fM has been achieved for DNA using an on-chip sandwich hybridization format, this is two orders of magnitude lower than the conventional fluorophore assay. In addition, the selectivity of our method is created at the DNA binding stage, wherein the cooperative behavior imparted by multiple DNA strands[11] on a single FNS allows for single-base mismatch discrimination using a facile salt-stringency wash.[3a,12] Further, our on-chip detection system also provides the ability to store and retrieve spatially resolved DNA sequence information and therefore allows for multiplexed detection of distinct DNA targets simultaneously.

[*] X. Shu, Y. Liu, Prof. Dr. J. Zhu
Department of Polymer Science and Engineering
School of Chemistry and Chemical Engineering
State Key Laboratory of Coordination Chemistry
Nanjing National Laboratory of Microstructures
Nanjing University, Nanjing, 210093 (China)
E-mail: jinz@nju.edu.cn

[**] J.Z. gratefully acknowledges support from the National Natural Science Foundation of China (21274058) and the National Basic Research Program of China (2013CB922101, 2011CB935801).

Supporting information for this article (experimental details) is available on the WWW under http://dx.doi.org/10.1002/anie.201205628.

The FNS assay system is comprised of two key components besides the target DNA: a DNA-derivatized FNS and a DNA-modified glass slide (Figure 1). The sequences of the DNA strands on the FNS and glass slide should be designed such that they form a contiguous, sandwich structure with the target DNA. As an initial test, a target sequence (**DNA3**, Supporting Information, Table S1) associated with the anthrax lethal factor[8] was selected for a proof-of-concept demonstration of the assay. For this target, an aminated DNA (**DNA1**, Table S1) and a thiolated DNA (**DNA2**, Table S1) were used to functionalize the FNS and the glass slide, respectively (Figure 1). One key to the successful implementation of our FNS method was the fabrication of a robust **DNA1**-modified FNS (**DNA1**-FNS). To this end, an approximately 96 nm FNS (Figure S1 A), with an EDAPS/Cu^{2+} ratio of 17.9:1,[9] was made that presents the amino groups of the EDAPS on the surface of the sphere. Conjugation of DNA was then carried out by reacting the amino groups on **DNA1** and the FNS with the aldehyde groups on bifunctional glutaraldehyde. The successful modification of FNSs with **DNA1** was confirmed by the change of ζ potential from $+38$ mV to -26.6 mV (Table S2). The as-prepared **DNA1**-FNS conjugate was treated with poly(vinylsulfuric acid) potassium salt (PVSK), and allowed to further react consecutively with sulfosuccinimidyl acetate and 2-(2-aminoethoxy)ethanol for the passivation of excess amino and aldehyde groups, respectively. The final **DNA1**-FNS probe (Figure S2 A), which was individually dispersed in 0.3 M phosphate-buffered saline (PBS) solution (0.3 M NaCl, 10 mM phosphate buffer, pH 7.0)/PVSK (2 mM)/sodium dodecyl sulfate (SDS, 0.1 wt%), as confirmed by dynamic light scattering measurements (Figures S1 B and S2 B), contains on average approximately 7.8×10^5 EDAPS and approximately 57 DNA molecules per sphere (Supporting Information). In principle, these numbers are sufficient to provide fluorescence signal amplification and single-base mismatch discrimination capabilities. The modification of glass slides with **DNA2** was performed using the following method: the hydroxy-rich glass slide was reacted initially with 3-aminopropyltriethoxysilane (APTES) and subsequently with succinimidyl 4-(*N*-maleimidomethyl)cyclohexane-1-carboxylate; excess amino groups were passivated with hexanoic anhydride; **DNA2** was coupled to the glass slide surface by reaction of the thiol group with the maleimido moiety; finally the excess maleimido groups were passivated with 1-hexanethiol.

With the two assay components assembled, we next evaluated the feasibility of our system for DNA detection. A glass slide spotted with **DNA2** was challenged in one-step with both target **DNA3** (1 μM, in 0.3 M PBS solution) and **DNA1**-FNS probe. The hybridization reaction enabled the surface confinement of the **DNA1**-FNS probe and formation of a grayish-blue spot at the **DNA2**-derivatized area (Figure 2 A). In either the absence of target **DNA3** or the presence of non-complementary **DNA4**, no signal could be detected. With the FNSs intact, no fluorescence could be observed under 365 nm UV irradiation owing to the highly effective quenching of the EDAPS signal by Cu^{2+} ions. By dissolving the FNSs and liberating the EDAPS in 0.5 μL *N*-butylmorpholine, a strongly fluorescent readout was produced (Figure 2 B). Pure EDAPS and the EDAPS released from the **DNA1**-FNS exhibit similar fluorescence spectra, with excitation maxima located at approximately 370 nm (Figures S3 and S4 A). The blue fluorescence signal could therefore be easily generated with a commercially available, handheld UV lamp (365 nm) and imaged with a digital camera to record the assay results. Additionally, it is important to understand the kinetics of FNS dissolution and the fluorescence generation. Thus, a **DNA1**-FNS sample was placed on a silicon wafer, dried, and incubated in *N*-butylmorpholine for various periods of time. Scanning electron microscopy revealed two key stages in the dissolution process, which took about eight minutes: 1) an initial change of the morphology from the spherical shape to a rod-like form and 2) a complete dissolution of the rod-like structure (Figure S5). Concomitant with the dissolution process was the emergence of the fluorescence signal, which plateaued within a short timeframe, as revealed by both fluorescence spectral measurement (Figure S4 B) and spot image analysis (Figure S6). The increase in fluorescence signal for a single-layer **DNA1**-FNS probe on a glass slide featured even faster kinetics, showing a plateau within two minutes. This quick fluorescence increase allows for a fast fluorescence readout. As expected, the fluorescence signal came only from the spot where target **DNA3** was present, thus demonstrating the effectiveness of the FNS assay.

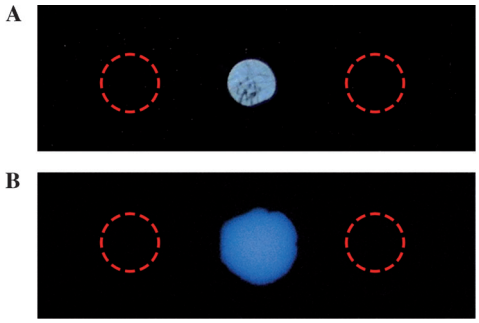

Figure 2. A) Macroscopic image of a glass slide in the absence of UV irradiation. Left to right: no target, **DNA3** (1 μM), and **DNA4** (1 μM) (spots with no fluorescence are designated by the dashed red circles). B) Macroscopic fluorescence image of a glass slide in the presence of 365 nm UV irradiation. Spots are identical to those in (A) except they were incubated in *N*-butylmorpholine.

Several observations from our initial optimization of the method are worth noting: 1) conjugation of **DNA1** with FNSs through another commonly used bifunctional molecule, 1,4-phenylene diisothiocyanate, was not successful because of the irreversible aggregation of FNSs under the basic reaction conditions that are required. 2) PVSK is required for the fabrication of **DNA1**-FNS probe in 0.3 M PBS solution. Without the protection of this anionic polyelectrolyte, the **DNA1**-FNS probe is not stable at such a high salt concentration. 3) APTES could not be substituted with 3-(2-aminoethylamino)propyltrimethoxysilane for the generation of surface amino groups. Otherwise, significant nonspecific adsorption of **DNA1**-FNS probe could be observed even in the absence of target **DNA3**. 4) The use of SDS is of

paramount importance at the **DNA1**-FNS probe hybridization stage. The pronounced background signal generated from a "coffee-ring stain",[13] as well as nonspecific adsorption, could be effectively nullified by the addition of SDS. 5) *N*-butylmorpholine is the solvent of choice for the assay because it has a high boiling point, low evaporation rate, high fluorescence quantum yield for EDAPS, and no photobleaching within the timeframe of the fluorescence readout.

This optimized method enables the minimization of background signal and thus allows us to fully explore the potential of the assay. One measure of the merit of a diagnostic system is the concentration dependence of the signal, which gives rise to two key assay attributes—dynamic range and detection limit. Thus, a glass slide spotted with a **DNA2** array was incubated with target **DNA3** of varied concentrations and the **DNA1**-FNS probe. At a target concentration of either 50 nM or 5 nM, the grayish blue spot formed by the FNSs could be clearly visualized (Figure S7), whereas the fluorescence readout can be detected at much lower concentrations (Figure 3A). Significantly, a monotonic concentration dependence of the fluorescence intensity

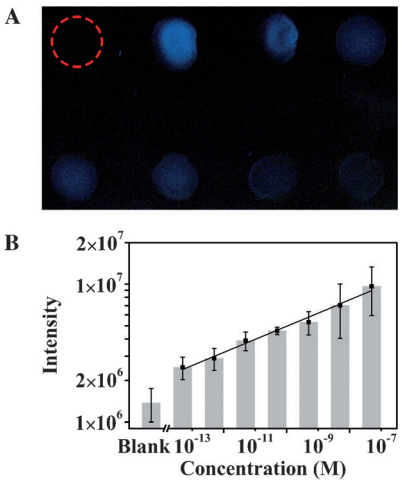

Figure 3. A) Macroscopic fluorescence image of a glass slide for the identification of **DNA3**. Target **DNA3** concentration (left to right, top to bottom): 0 M, 50 nM, 5 nM, 0.5 nM, 50 pM, 5 pM, 0.5 pM, and 50 fM. B) Fluorescence intensity as a function of **DNA3** concentration (note the logarithmic scale). Error bars indicate the standard deviation calculated from three independent experiments. Background signal for a sample with no DNA target: 1.37×10^6.

(through either direct visualization, Figure 3A or blue channel brightness readout, Figure 3B) was clearly observed. If plotted on a double logarithmic scale, a linear relationship exists across a concentration range of six orders of magnitude, indicating a wide dynamic range and good quantification capability (Figure 3B). With this assay, a 50 fM target could be unambiguously visualized against the essentially zero background, which translates to a detection limit of 100 zmol (2 μL). The detection limit was also validated using blue channel brightness, by virtue of consistently low background signal, under either high (Figure 3B) or low (Figure 4B, see below) salt concentration. In principle, using larger FNSs

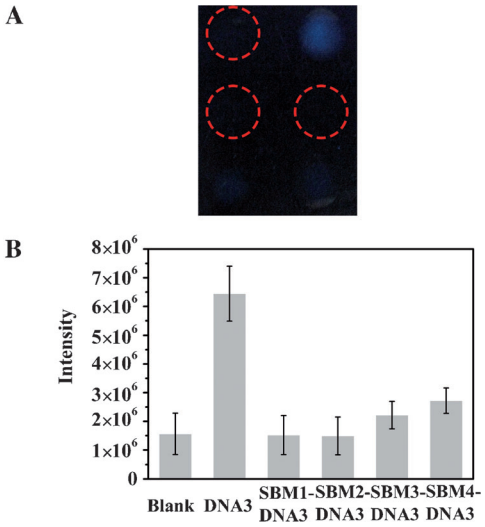

Figure 4. A) Macroscopic fluorescence image of a glass slide for single-base mismatch discrimination. Left to right, top to bottom: no DNA target, **DNA3**, **SBM1-DNA3**, **SBM2-DNA3**, **SBM3-DNA3**, and **SBM4-DNA3**. B) Fluorescence intensity for each of the spots in (A) (note the linear scale). Background signal for a sample with no DNA target: 1.56×10^6.

could provide a more pronounced signal amplification and therefore allow for further improvement in the sensitivity of the assay.

An assay that can discriminate single-base mismatches is important for screening for genetic diseases. Both a thermal-stringency wash[3a,11] (with elevated temperature) and salt-stringency wash[3a,12] (with lower salt concentration) have been developed as methods for single-base mismatch discrimination through selective, preferential de-hybridization of less thermodynamically stable mismatched hybrids compared to a perfect-match hybrid. As the **DNA1**-FNS probe has about 57 DNA molecules per sphere, cooperative binding behavior should enable the facile distinction of DNA strands.[3a,11] As a demonstration of the selectivity of our assay, a perfect-match target and DNA strands with different single-base mismatch features (**SBM1-DNA3**, mismatch at middle; **SBM2-DNA3**, insertion; **SBM3-DNA3**, deletion; **SBM4-DNA4**, mismatch at end) were tested. A salt-stringency wash was employed to avoid the challenge of an on-chip temperature control setup.[8a] Indeed, at a salt concentration of 7.5 mM (PBS: 7.5 mM NaCl, 0.75 mM phosphate buffer, pH 7.0), the **DNA1**-FNS probe incubated with the mismatched strands exhibited much lower fluorescence signal as compared with the perfect-match target, showing the good mismatch discrimination of the method (Figure 4). Note that for typical target DNA detection (Figure 3), a higher salt concentration is routinely used,[3a] because closely related, mismatched strands are generally absent.

The on-chip assay format associated with our detection system could allow for spatially resolved parallel storage of DNA sequence information and therefore enable multiplexed detection of distinct DNA targets.[14] As a demonstration of the ability to perform multiplexed analysis, a two-target sample (**DNA3** and **DNA7**) was subjected to the assay. To

achieve this, a DNA chip was spotted with both **DNA2** and **DNA6**, and a second probe, **DNA5**-FNS, was fabricated. Analogously, the sequences of **DNA6** and **DNA5** were selected such that they could form a sandwich hybrid with **DNA7**. The multiplexed analysis proceeds in a background-free manner similar to the single-target case. Thus, **DNA1**-FNS and **DNA5**-FNS probes were captured to the corresponding DNA spots only in the presence of their respective targets. At higher DNA concentrations, the captured FNS probes could be visualized either in the intact form (Figure S8) or in fluorescence mode (Figure 5), and the two

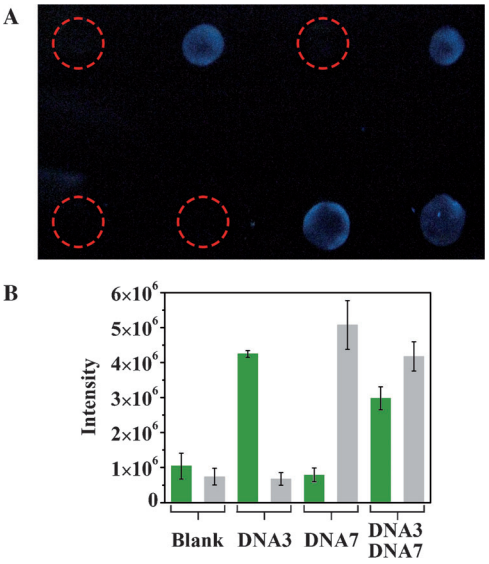

Figure 5. A) Macroscopic fluorescence image of a glass slide for the identification of two DNA targets. Left to right: no DNA target, **DNA3**, **DNA7**, and both **DNA3** and **DNA7**. Top row: modified with **DNA2** and challenged with **DNA1**-FNS probe. Bottom row: modified with **DNA6** and challenged with **DNA5**-FNS probe. The concentration of each target was 10 nM. B) Fluorescence intensity for each of the spots in (A). Green: fluorescence intensity for the top row. Gray: fluorescence intensity for the bottom row.

targets could be readily distinguished. At lower concentrations, the two targets could only be detected using the fluorescence approach (Figure S9). It should be noted that, although only sparsely distributed spots were generated and each spot was individually addressed in this proof-of-concept demonstration, spot miniaturization and parallel detection can be easily achieved for our assay owing to the localized FNS dissolution process, smaller droplet sizes that can be automatically and precisely dispensed,[15] and an exquisite fluorescence spot detector that has been developed for gene chip technology.[16]

In summary, a DNA detection strategy based on FNSs has been developed. The assay features a latent FNS fluorophore probe, which gives signal amplification through the release of multiple fluorophores. The complete division between DNA hybridization and signal generation allows for simultaneous high selectivity and high sensitivity. This on-chip assay provides the ability to perform multiplexed analysis in an array format. The detection scheme reported herein should be applicable to a broad range of targets by virtue of the generic fluorescent signal generated by the FNS probe.

Received: July 16, 2012
Published online: September 28, 2012

Keywords: DNA detection · fluorescent probes · fluorogenic nanospheres · nanoparticles · signal amplification

[1] a) D. A. Giljohann, C. A. Mirkin, *Nature* **2009**, *462*, 461 – 464; b) P. Scrimin, L. J. Prins, *Chem. Soc. Rev.* **2011**, *40*, 4488 – 4505; c) A. Sassolas, B. D. Leca-Bouvier, L. J. Blum, *Chem. Rev.* **2008**, *108*, 109 – 139; d) L. Zhu, E. V. Anslyn, *Angew. Chem.* **2006**, *118*, 1208 – 1215; *Angew. Chem. Int. Ed.* **2006**, *45*, 1190 – 1196; e) J. Liu, Z. Cao, Y. Lu, *Chem. Rev.* **2009**, *109*, 1948 – 1998.
[2] a) R. K. Saiki, S. Scharf, F. Faloona, K. B. Mullis, G. T. Horn, H. A. Erlich, N. Arnheim, *Science* **1985**, *230*, 1350 – 1354; b) G. M. Makrigiorgos, S. Chakrabarti, Y. Zhang, M. Kaur, B. D. Price, *Nat. Biotechnol.* **2002**, *20*, 936 – 939; c) M. T. Dorak, *Real-Time PCR*, Taylor & Francis, New York, **2006**.
[3] a) N. L. Rosi, C. A. Mirkin, *Chem. Rev.* **2005**, *105*, 1547 – 1562; b) B. W. Kirk, M. Feinsod, R. Favis, R. M. Kliman, F. Barany, *Nucleic Acids Res.* **2002**, *30*, 3295 – 3311.
[4] L. Cartechini, M. Vagnini, M. Palmieri, L. Pitzurra, T. Mello, J. Mazurek, G. Chiari, *Acc. Chem. Res.* **2010**, *43*, 867 – 876.
[5] R. M. Lequin, *Clin. Chem.* **2005**, *51*, 2415 – 2418.
[6] W. H. Scouten, J. H. T. Luong, R. S. Brown, *Trends Biotechnol.* **1995**, *13*, 178 – 185.
[7] Y. C. Cao, R. Jin, C. A. Mirkin, *Science* **2002**, *297*, 1536 – 1540.
[8] a) X. Zhou, S. Xia, Z. Lu, Y. Tian, Y. Yan, J. Zhu, *J. Am. Chem. Soc.* **2010**, *132*, 6932 – 6934; b) X. Zhou, P. Cao, Y. Tian, J. Zhu, *J. Am. Chem. Soc.* **2010**, *132*, 4161 – 4168; c) M. Hong, X. Zhou, Z. Lu, J. Zhu, *Angew. Chem.* **2009**, *121*, 9667 – 9670; *Angew. Chem. Int. Ed.* **2009**, *48*, 9503 – 9506; d) F. Qiu, D. Jiang, Y. Ding, J. Zhu, L. L. Huang, *Angew. Chem.* **2008**, *120*, 5087 – 5090; *Angew. Chem. Int. Ed.* **2008**, *47*, 5009 – 5012; e) Y. Yan, W. Sha, J. Sun, X. Shu, S. Sun, J. Zhu, *Chem. Commun.* **2011**, *47*, 7470 – 7472.
[9] X. Shu, Z. Lu, J. Zhu, *Chem. Mater.* **2010**, *22*, 3310 – 3312.
[10] a) X. Liu, X. Shu, X. Zhou, X. Zhang, J. Zhu, *J. Phys. Chem. A* **2010**, *114*, 13370 – 13375; b) J.-S. Yang, S.-Y. Chiou, K.-L. Liau, *J. Am. Chem. Soc.* **2002**, *124*, 2518 – 2527; c) J.-S. Yang, K.-L. Liau, C.-M. Wang, C.-Y. Hwang, *J. Am. Chem. Soc.* **2004**, *126*, 12325 – 12335; d) J.-S. Yang, K.-L. Liau, C.-Y. Li, M.-Y. Chen, *J. Am. Chem. Soc.* **2007**, *129*, 13183 – 13192.
[11] J. I. Cutler, E. Auyeung, C. A. Mirkin, *J. Am. Chem. Soc.* **2012**, *134*, 1376 – 1391.
[12] S. J. Park, T. A. Taton, C. A. Mirkin, *Science* **2002**, *295*, 1503 – 1506.
[13] a) R. D. Deegan, O. Bakajin, T. F. Dupont, G. Huber, S. R. Nagel, T. A. Witten, *Nature* **1997**, *389*, 827 – 829; b) H. Hu, R. G. Larson, *J. Phys. Chem. B* **2006**, *110*, 7090 – 7094.
[14] a) R. F. Service, *Science* **1998**, *282*, 396 – 399; b) J. Wang, *Nucleic Acids Res.* **2000**, *28*, 3011 – 3016.
[15] D. T. Chiu, R. M. Lorenz, *Acc. Chem. Res.* **2009**, *42*, 649 – 658.
[16] D. J. Lockhart, E. A. Winzeler, *Nature* **2000**, *405*, 827 – 836.